ISSN 1330-3651
UDC/UDK 543.42:[62-408:621.9.044.4]

# SPECTRAL ANALYSIS OF METALLIC SURFACES TOPOGRAPHY GENERATED BY ABRASIVE WATERJET

***Kateřina Brillová, Miloslav Ohlídal, Jan Valíček, Dražan Kozak, Sergej Hloch, Michal Zeleňák, Marta Harničárová, Petr Hlaváček***

Original scientific paper

A basic study of a surface topography generated by an abrasive waterjet cutting is performed by means of the spectral analysis of these surfaces. The initial data were acquired by using an optical profilometer MicroProf FRT in the form of 2D maps of the surfaces' heights. The basic notions of the spectral analysis applied to the surface topography are presented. Limitations of the measurement procedure are considered. Distortions of the areal power spectral density are discussed. An estimation of the areal power spectral density is carried out using a periodogram method combined with the Welch´s method. A comparison of surfaces prepared by the abrasive waterjet cutting with different values of the cutting technological parameters is performed. It has been demonstrated that the areal spectral analysis of the aforementioned surfaces offers new possibilities of their topography characterization.

***Keywords:*** *abrasive waterjet cutting, spectral analysis, surface topography*

## Spektralna analiza topografije metalnih površina stvorenih pomoću abrazivnog vodenog mlaza

Izvorni znanstveni članak

Osnovna studija topografije površina nastalih rezanjem abrazivnim vodenim mlazom izrađena je uz pomoć spektralne analize tih površina. Početni podatci su prikupljeni primjenom optičkog profilometra MicroProf FRT u obliku 2D karata visina površina. U radu se predstavljeni osnovni pojmovi spektralne analize primijenjeni na topografiju površine. Razmotrena su ograničenja postupka mjerenja. Raspravljena su iskrivljavanja površinske gustoće spektra snage. Procjena površinske gustoće spektra snage je obavljena pomoću metode periodograma u kombinaciji s Welchovom metodom. Uspoređene su površine dobivene rezanjem pomoću abrazivnog vodenog mlaza uz različite vrijednosti tehnoloških parametara rezanja. Pokazano je da se spektralnom analizom navedenih površina nude nove mogućnosti karakterizacije njihove topografije.

***Ključne riječi:*** *rezanje abrazivnim vodenim mlazom, spektralna analiza, topografija površine*

## 1 Introduction

Development and applications of new materials in mechanical engineering practice bring a lot of questions concerning their technological treatment. Nowadays classical machining of these materials is complemented by new technologies. The machining of materials by an abrasive waterjet (AWJ) represents one of such relatively new and progressive methods. AWJ offers a versatile flexible tool to allow machining of all natural and artificial materials which may get in contact with water. A wide range of such materials brings a lot of unanswered problems concerning their mutual interaction with the AWJ. The first pioneering works in this field were accomplished by Hashish [6] who studied the influence of technological parameters on the depth of cutting profile. He also proposed a mathematical model for the prediction of the maximum depth of the cut. A great deal of attention was paid to a study of the surface topography of cutting walls generated by AWJ. A study of the surface topography is important for AWJ modelling and prediction. A mechanism of the AWJ stock removal is still a poorly studied field of the AWJ technology. A disintegration of materials by means of AWJ involves a mechanism of cutting, plastic deformation, fatigue and fracture of those materials. Due to the investigation of the surface topography generated by the AWJ machining process it is possible to gain a better understanding of this process; to specify its theory and to quantify correctly the AWJ stock removal mechanism [7–10]. Surfaces generated by means of AWJ machining show a characteristic topography. The picture of a surface (see Fig. 1) includes specific zones, namely the initiation zone, smooth zone, transition zone and rough zone. The surface has four topographical different zones with different values of surface parameters *Ra*, *Rq*, *Rz* [1–*5*].

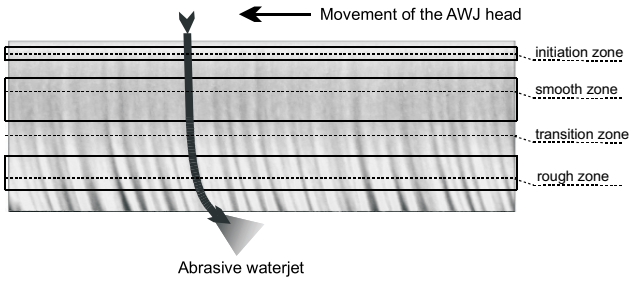


**Figure 1** Individual zones within a surface generated by AWJ cutting

## 2 Experiments

Investigated surfaces generated by AWJ cutting were prepared from 10-mm thick steel plates (material AISI 304) of size 300×50×10 $mm^3$. The schematic diagram of the cutting AWJ head used in experiment is presented in Fig. 2. Ultra high - pressure water goes through the water nozzle into the inlet chamber where it is mixed together with the garnet abrasive. The abrasive waterjet is formed in the cutting nozzle and interacts with the upper surface of sample, which is perpendicular to the abrasive waterjet. The constant parameters of the AWJ cutting were: Jet diameter = 0,1 mm, focusing tube diameter = 1 mm, abrasive grain size 80 MESH, nozzle–surface distance = 3 mm.

Several AWJ cutting technological parameters of the surface preparation were selected to observe their influence on the surface topography. These parameters were the following: the pressure of water on the input of the cutting AWJ head, the traverse speed of the AWJ head and the abrasive flow rate.

The values of the AWJ cutting technological parameters being changed are presented in Tab. 1.

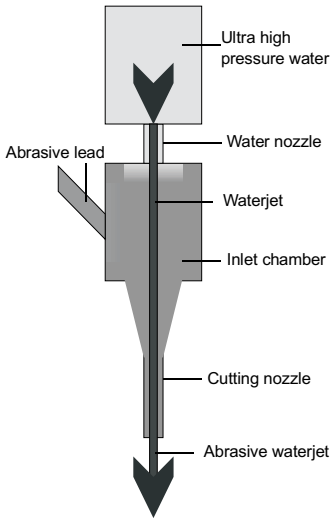


**Figure 2** Schematic view of AWJ cutting head

**Table 1** Experimental conditions of AWJ

| Factors | Sign | Unit | Value |
|---|---|---|---|
| Pressure on the input of cutting head | $p$ | MPa | 200 and 350 |
| Traverse speed | $v$ | mm/min | 70 and 120 |
| Abrasive mass flow rate | $m_a$ | g/min | 350 and 500 |
| Abrasive size | - | MESH | 80 |
| Abrasive material | Australian garnet GMA | | |

## 3
## Topography measurement

The aforementioned surfaces were measured by using an optical profilometer (Fig. 3). This profilometer MicroProf FRT enabled us to obtain a map of the surface heights with regard to a reference plane. It is useful for 3D surface topography assessment. The principle of the optical profilometer operation is based on utilization of chromatic aberration of the positive lens of the optical sensor CHR 150 N (Fig. 4). White light from a halogen bulb goes through the positive lens with high chromatic aberration. Different light monochromatic components are focused in different heights from the reference plane at the output of the optical fibre. The same optical fibre collects scattered light from the surface under study. This light is analysed by means of a spectrometer. The light is best captured when focused on the surface. It means that the spectral intensity distribution of the light being processed by the spectrometer has a maximum at a wavelength of a monochromatic component exactly focused on the surface. The height of the surface irregularities is deduced by means of a calibration table from the wavelength of the spectral distribution of maximum intensity. The optical sensor is non-movable, the sample under study lies on a scanning table.

The same optical fibre collects scattered light from the surface under study. This light is analysed by means of the spectrometer. The results of the measurement have the form of a vector and/or the matrix of heights of the surface irregularities. The basic parameters of MicroProf FRT are as follows: minimal range $xy$ : 200 × 200 μm$^2$, maximal range $xy$ : 100 × 100 mm$^2$, measurement range $z$: 300 μm – 3 mm, vertical resolution: 3 nm, lateral resolution: 2 μm, maximum angle of inclination of the surface roughness to the mean plane: 30°.

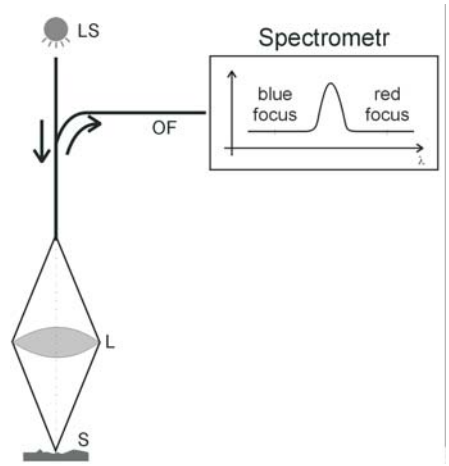


**Figure 3** LS – halogen bulb, OF – optical fibre, L – positive lens of the sensor CHR 150 N, S – sample under study, Spectrometer – micro-spectrometer

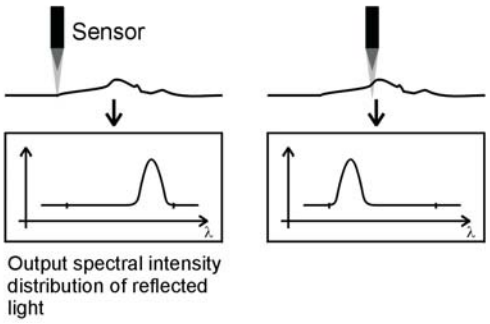


**Figure 4** Different light monochromatic components are focused in different heights from a reference plane at the output of the optical fibre

## 4
## Spectral analysis of surface topography

Spectral analysis of a surface topography provides a special view of the surface topography characterization. Analysis of the topography in the frequency domain makes it possible to accentuate some surface topography features which are noticeable worse within the spatial domain. It is interesting to apply the spectral analysis to surfaces generated by AWJ cutting. These surfaces are of a random character (the detailed specification can be found in [13]). The process of their topography measurement provides individual realization of a 2D random function which represents the surface under study (so called surface function). This function is non-stationary within its complete extent. As already mentioned in the introduction, it is possible to select the individual zones of the surface in which the surface function can be considered as a stationary function (i.e. there is not any change of the surface character within the whole individual zone) and ergodic (i.e. it is possible to evaluate the features of the whole surface topography within the individual zone from an individual sufficiently large surface realization within the zone) 2D random function. Considering the surface under study as the random function it is necessary to describe the surface by means of the mean quantities derived from an amplitude of Fourier's spectrum realization or, as usually, from the squares of these spectra in the frequency domain. These squares of Fourier spectra are called the energy or power spectra of surface realization. The expected value (mean) *of* Fourier transforms of individual surface realizations usually tends to zero function identically due to the

distribution of their phases. Thus, the mean of these Fourier transforms does not provide any information.

A non-limited (i.e. defined along the whole plane $x$, $y$) realization of the random surface under study by the surface function $z = z(x, y)$ in the coordinate system O$xyz$ will be described, where $z$ is the surface height with respect to the plane $x$, $y$ at the point $[x, y]$. Hence, the function $z = z(x, y)$ is the realization of a stationary and ergodic random function $z_r = z(x, y)$ selected by a process of measurement. The function $z = z(x, y)$ is defined along the whole plane $x$, $y$. But information on the function of $z = z(x, y)$ is acquired only from a finite region $X$, $Y$ of the plane $x$, $y$ by the MicroProf FRT profilometer measurement. So, it is necessary to deal with the function $Z_{X,Y} = Z_{X,Y}(x, y)$ defined as follows:

$$Z_{X,Y}(x,y) = z(x,y) \quad \text{for} \quad |x| \le X \wedge |y| \le Y \tag{1}$$
$$z_{X,Y}(x,y) = 0 \quad \text{otherwise.}$$

This function has the Fourier integral

$$Z_{X,Y}(f_x, f_y) = \int_{-\infty}^{\infty}\int_{-\infty}^{\infty} z_{X,Y}(x,y)\exp\left[-i2\pi(f_x x + f_y y)\right]\mathrm{d}x\,\mathrm{d}y. \tag{2}$$

Then it is possible to define the areal power spectral density (APSD) of the function $z = z(x, y)$ as follows (Remark: The expression areal power spectrum is used for this quantity in literature alternatively):

$$P(f_x, f_y) = \lim_{\substack{X\to\infty \\ Y\to\infty}} \left[\frac{|Z_{X,Y}|^2}{XY}\right]. \tag{3}$$

APSD of the whole random function $z_r$ is defined as:

$$P_{zr}(f_x, f_y) = \lim_{\substack{X\to\infty \\ Y\to\infty}} \left[\frac{\left\langle |Z_{X,Y}|^2 \right\rangle}{XY}\right], \tag{4}$$

where the symbol $\langle\ \rangle$ denotes the mean of the surface realizations population. The quantity $P_{ZY}(f_x, f_y)$ indicates in what way the mean power of the studied surface is distributed within the frequency domain. This quantity will be used for the characterization of surfaces generated by AWJ. The characterization of the surface topography within these zones along an individual surface profile can be performed by means of a frequency-amplitude analysis (2D surface evaluation) [12]. A more advanced approach is the surface topography characterization by means of the discrete fast Fourier transform (DFFT) [11, 12] of 2D data (maps of surface heights) within these zones (in accordance with the technical practice so called 3D evaluation of surfaces is performed). Of course it is possible to base the spectral analyses on other transforms. The aim of the work presented is to find the characteristic features of the surface within the individual zones by means of this technique, to link them to the technological parameters of the surface preparation and to obtain their relationship to the mechanism of the surface generation during the cutting of materials by AWJ. According to our best knowledge the application of the areal data spectral analysis has not been used yet for the topography characterization of the surfaces generated by the AWJ cutting. More detailed quantitative description of a random function within the frequency domain is allowed by the following quantities derived from APSD of the function. These are angular power spectral density (AnPSD) and radial power spectral density (RPSD) of the function. It is possible to characterize the shape of APSD, i.e. the distribution of the random function power within the frequency plane by means of both [13]. To define these quantities it is necessary to transform the APSD (see Eq. 4) into polar coordinates within the frequency domain

$$P_{zr}(f_x, f_y) \to P_{zr}(f_r, \theta), \text{ where}$$

$$f_x = f_r\cos\theta,\ f_y = f_r\sin\theta,\ f_r = \sqrt{f_x^{\,2} + f_y^{\,2}},\ \theta = \arctan\left(\frac{f_y}{f_x}\right).$$

Then AnPSD is defined as follows [13]:

$$P_\theta(\theta) = \int_0^{f_{r\max}(\theta)} P(f_r, \theta)\,\mathrm{d}f, \tag{5}$$

where $0 \le \theta \prec \pi$ and $f_{r\max}(\theta)$ is a maximum frequency contained within the cross-section of APSD given by the angle $\theta$. A Distribution of the power of the studied random function along the individual directions within the frequency plane can be described by this quantity. RPSD is defined as follows [13]:

$$P_{f_r}(f_r) = \int_0^{179} P(f_r, \theta)\mathrm{d}\theta, \tag{6}$$

where $0 \le f_r \le \min\{f_{X\max}, f_{Y\max}\}$. RPSD describes the distribution of the power in the frequency domain of the studied random function components. It neglects the orientation of these components.

### 4.1 Limitations of measuring procedure

The measurement of the studied surface heights by the optical profilometer MicroProf FRT provides a discrete form of the function $Z_{X,Y}(x,y)$, i.e. the sampled function $Z_{X,Y}(x_m,y_n)$, where $m \in 0...M-1$, $n \in 0...N-1$, $m$, $n$ are integers. The surface of the sample in the squared grid of equidistant points, i.e. $M=N$, is usually measured. It is obvious that the integral Fourier transform $Z_{X,Y}(f_x,f_y)$ of the continuous function $Z_{X,Y}(x,y)$ must be replaced by the discrete Fourier transform $\widetilde{Z}_{X,Y}(f_k,f_l)$ of the sampled function $Z_{X,Y}(x_m,y_n)$. It is defined as follows:

$$\widetilde{Z}_{X,Y}\left(\frac{k}{M\,\Delta x}, \frac{l}{N\,\Delta y}\right) = \sum_{m=0}^{M-1}\sum_{n=0}^{N-1} z_{X,Y}(m\,\Delta x, n\,\Delta y)\exp\left[-i2\pi\left(\frac{k}{M}m + \frac{l}{N}n\right)\right] \tag{7}$$

where $0 \le k \le M-1$; $0 \le k \le N-1$, $\Delta x$ is the sampling interval along the $x$ axis, $\Delta y$ is the sampling interval along the $y$ axis, $k/(M\,\Delta x)$ is the $l^{\text{th}}$ value of the spatial frequency along the $f_x$ axis, $l/(N\,\Delta y)$ is the $l^{\text{th}}$ value of the spatial frequency along the $f_y$ axis. The function $\widetilde{Z}_{X,Y}$ is used to determine $P(f_x,f_y)$ in

Eq. (3). Nevertheless a distortion in this procedure is necessarily committed, the cause of which is as follows:

- The limit transition in Eq. (3) supposes a possibility to enlarge the $X$, $Y$ region (where the topography of the surface is measured) without any stint. But the surface topography can be measured only from a limited region $X$, $Y$ of the surface.
- The sampled discrete function is used.

$$z_{X,Y}(x_m, y_n) = \\ = z_{X,Y}(x,y) \sum_{m=-\infty}^{\infty} \delta(x - m\Delta x) \sum_{n=-\infty}^{\infty} \delta(y - n\Delta y) \tag{8}$$

instead of the continuous function $Z_{X,Y}(x,y)$ from Eq. (2). Meaning of symbols in Eq. (8) is as follows:

- $\sum_{m=-\infty}^{\infty} \delta(x - m\Delta x)$ is the sequence of the Dirac distributions displaced with a step $\Delta x$ along the $x$ axis,
- $\sum_{n=-\infty}^{\infty} \delta(y - n\Delta y)$ is the sequence of the Dirac distributions displaced with a step $\Delta y$ along the $y$ axis.

### 4.2 Discussion of APSD distortions

Let us discuss these distortions. The surface topography is measured within the finite region described by Eq. (1). The surface function can be written within this region as follows:

$$z_{X,Y}(x,y) = z(x,y)\,\mathrm{rect}\left(\frac{x}{X}\right)\mathrm{rect}\left(\frac{y}{Y}\right), \tag{9}$$

where the truncation function

$$\mathrm{rect}\left(\frac{x}{X}\right)\mathrm{rect}\left(\frac{y}{Y}\right)$$

is defined in the following way:

$$\begin{aligned} &\mathrm{rect}\left(\frac{x}{X}\right)\mathrm{rect}\left(\frac{y}{Y}\right) = 1 \quad |x| \prec X \wedge |y| \prec Y \\ &\mathrm{rect}\left(\frac{x}{X}\right)\mathrm{rect}\left(\frac{y}{Y}\right) = 1/2 \quad |x| = X \wedge |y| = Y \\ &\mathrm{rect}\left(\frac{x}{X}\right)\mathrm{rect}\left(\frac{y}{Y}\right) = 0 \quad \text{otherwise.} \end{aligned} \tag{10}$$

Product in Eq. (9) leads to a convolution of the Fourier transform of the function $z(x,y)$ (this Fourier transform exists in a generalized sense of the Fourier transform within the limit) and also the Fourier transform of the function $\mathrm{rect}(x/X)\mathrm{rect}(y/Y)$, i.e. the function $|X||Y|\,\mathrm{sinc}(Xf_x)\,\mathrm{sinc}(Xf_y)$. Because of the finite extent of the definition domain of the function $\mathrm{rect}(x/X)\mathrm{rect}(y/Y)$ this convolution leads to a distortion of the Fourier transform of the function $z(x,y)$ being sought. This distortion gives rise to nonzero components of the spectrum in new frequencies. It is so called the leakage spectrum in these new incorrect frequencies. This phenomenon can be suppressed by a selection of the largest possible domain of definition $X$, $Y$ of the function $\mathrm{rect}(x/X)\mathrm{rect}(y/Y)$, i.e. the region of the surface topography measurement. Another possibility suppressing the leakage of the spectrum is to use another more appropriate function – so called weighting function $w(x,y)$ (e.g. Hann function – see below) instead of the function $\mathrm{rect}(x/X)\mathrm{rect}(y/Y)$ in Eq. (9). Then so called weighting the function $z(x,y)$ by the data-weighting function $w(x,y)$ is carried out. Further consequence of the aforementioned convolution is a smearing or blurring of the Fourier transform of the function $z(x,y)$. Of course, the less frequency smears, the better the frequency-resolving power is possible. It is possible to decrease the frequency smear by the selection of a wider truncation function. In that case the function $|X||Y|\,\mathrm{sinc}(Xf_x)\mathrm{sinc}(Xf_y)$ is narrower and its convolution with the function $Z_{X,Y}(f_x,f_y)$ shows the lower frequency smear. As it can be seen from Eq. (7), the size of the region $X = M\Delta x$, $Y = N\Delta y$ influences also the resolution (i.e. the sampling interval) within the frequency domain. An increase in $X$ or $Y$ leads to a decrease of the sampling intervals $\Delta f_x$, $\Delta f_y$ in adequate frequencies $f_x$, $f_y$, i.e. the resolution in the frequency domain improves. The size of the region $X$, $Y$ can be regulated in two ways. One of them is the selection of the sampling intervals $\Delta x$, $\Delta y$ of the function $z_{X,Y}(x,y)$ within the spatial domain, and the second one is the selection of the values of the numbers $M$, $N$. The first of the aforementioned possibilities is limited by the Nyquist theorem in the case of frequency – limited functions (maximum frequencies $\Delta f_{x\max}$, $\Delta f_{y\max}$ exist within the spectrum of these functions. The functions obtained from the measuring process are frequency-limited in practice since a measuring apparatus records the frequencies only up to the certain maximum values given by the construction of an apparatus or the measuring method used by the apparatus). According to this theorem it is necessary to select the sampling intervals as $\Delta x \leq 1/2f_{x\max}$ and $\Delta y \leq 1/2f_{y\max}$ to avoid the distortion of the Fourier transform caused by aliasing. In the case of the frequency non-limited functions it is possible only to minimize this distortion by the selection of the lowest possible sampling intervals $\Delta x$, $\Delta y$ or by using an anti – aliasing filter as a function of pre-processing. The choice of the lowest possible sampling intervals $\Delta x$, $\Delta y$ increases the sampling interval within this spectrum and thus it decreases the resolution within the frequency domain. Hence it is necessary to choose the utmost possible values of $M$, $N$ (numbers of samples of the function under study) for the given values of the sampling intervals $\Delta x$, $\Delta y$ (considering the Nyquist theorem) to increase this resolution within the frequency domain. Of course when doing it in this way, there is a limit given by a maximum data range which can be processed by a computer still effectively. It is obvious from the aforementioned in what way the limitation and the sampling of the measured surface distort the sought spectrum of the function $z(x,y)$. Necessarily the areal spectrum power density $P(f_x,f_y)$ in the Eq. (3) is also distorted.

### 4.3 Periodogram APSD estimation

Hitherto the individual finite realization of the random function $z_r = z(x,y)$ has been discussed. The ASPD of the whole random function $z_r$ is given by the Eq. (4). It is again valid that, in principle, it is not possible to accomplish the limit transition in the Eq. (4) to the infinite region $X$, $Y$ of the

plane $x, y$. It is not also possible to find $\langle|Z_{X,Y}|^2\rangle$ because it is not possible to analyse an infinite number of possible realizations of the function $z_r$. These two reasons lead to the fact that the result must be only an estimate of the APSD from the Eq. (4). The mean value $\langle|Z_{X,Y}|^2\rangle$ can be estimated in the Eq. (4) from a finite number of realizations of the random function $z_r$ as the arithmetic average

$\frac{1}{Q}\sum_{q=1}^{Q}\left|Z_{X,Y,q}\right|^2$, i.e. the following approximation is used:

$$\left\langle\left|Z_{X,Y,q}\right|^2\right\rangle \cong \frac{1}{Q}\sum_{q=1}^{Q}\left|Z_{X,Y,q}\right|^2. \tag{11}$$

Hence, it is possible to express approximately the Eq. (4) as follows:

$$P_{zr}\left(\frac{k}{M\Delta x},\frac{l}{N\Delta y}\right)\cong\frac{1}{Q}\sum_{q=1}^{Q}\left[\left|\frac{Z_{X,Y,q}\dfrac{k}{M\Delta x},\dfrac{l}{N\Delta y}}{MN\Delta x\Delta y}\right|^2\right] \tag{12}$$

where $0 \le k \le M-1$; $0 \le k \le N-1$. Using the relation (12) so called periodogram method of the determination of the ASPD estimation of the random function $z_r$ is employed.

### 4.4
### Welch's method

The calculation on the right side of the Eq. (12) can be carried out in several ways. The Welch´s method has been selected because only one finite discrete realization $z_{X,Y}(x_m,y_n)$ of the random function $z_r$ is available. This method is based on the assumption that the relevant function $z_r$ is ergodic, i.e. the measured realisation $z_{X,Y}(x_m,y_n)$ provides representative information about the whole random function $z_r$. Within the framework of this method the measured domain of the given realisation is resolved into a sufficient number of the mutually overlapping sub-domains $z_{X',Y'}(x_{m'},y_{n'})$. As the next step of the Welch´s method weighting the surface function in each sub-domain by a chosen weighting function $w(x_{m'},y_{n'})$ was carried out. The following expression for each weighted sub-domain denoted by the indices $q'$ was determined:

$$\frac{\left|Z_{w,X',Y',q'}\left(\dfrac{k}{M'\Delta x},\dfrac{l}{N'\Delta y}\right)\right|^2}{M'N'\Delta x\,\Delta y} \tag{13}$$

for $0 \le k \le M'-1; 0 \le l \le N'-1, M' \prec M, N' \prec N$

The symbol $Z_{w,X',Y',q'}\left(\dfrac{k}{M'\Delta x},\dfrac{l}{N'\Delta y}\right)$ in the expression (13) denotes the Fourier transform of the surface function weighted by the function $w(m'\Delta x, n'\Delta y)$ within the selected $q'^{\text{th}}$ domain $X'$, $Y'$. The resolution within the frequency domain is again decreased by the selection of $M' \prec M$, $N' \prec N$ in the Eq. (13) and simultaneously an undesired smoothing of the APSD estimations from the individual sub-domains accompanied by the improved leakage of the adequate spectra is performed. In conclusion the arithmetic average of the $Q'$ spectra of the weighted surface function within the all sub-domains was calculated:

$$\overline{P}_W=\frac{1}{Q'}\sum_{q=1}^{Q'}\frac{\left|Z_{w,X',Y',q'}\left(\dfrac{k}{M'\Delta x},\dfrac{l}{N'\Delta y}\right)\right|^2}{M'N'\Delta x\,\Delta y}. \tag{14}$$

Considering the assumption of the function $z_r$ ergodicity the term (14) is equivalent to the arithmetic average of the given number of finite realizations of $z_r$. The term (14) is the resulting statistical estimate of the APSD defined by the Eq. (4). Hence

$$P_{zr}\left(\frac{k}{M'\Delta x},\frac{l}{N'\Delta y}\right)\cong$$
$$\cong\overline{P}_W\left(\frac{k}{M'\Delta x},\frac{l}{N'\Delta y}\right)=\frac{1}{Q'}\sum_{q-1}^{Q'}\frac{\left|Z_{w,X',Y',q'}\left(\dfrac{k}{M'\Delta x},\dfrac{l}{N'\Delta y}\right)\right|^2}{M'N'\Delta x\,\Delta y}. \tag{15}$$

It is obvious that the dispersion of the resulting estimate $\overline{P}_W$ of the ASPD was decreased by increasing the number of sub-domains used in averaging on the one hand, but simultaneously the resolution within the frequency domain was decreased by reducing the sub-domains size on the other hand. Thus the information about the details of the averaged APSD shape was lost. The choice of the domains size and the number of them is a question of a compromise.

The estimate $\overline{P}_W\left(\dfrac{k}{M'\Delta x},\dfrac{l}{N'\Delta y}\right)$ of the APSD of the surface under study gives an interesting view about the typical features of this surface (see below). As regards the discrete form of terms (5) and (6) for the APSD and RPSD an appropriate numerical algorithm for their calculation was used.

## 5
## Results and discussion

The surface topography was measured within the one-piece region of 6 × 2 mm$^2$ inside the individual zones. 18 overlapping sub-domains (with a 50 % overlap) with a size of 0,6 × 0,6 mm$^2$ ($M' = N' = 300$ were used for estimation of $\overline{P}_W\left(\dfrac{k}{M'\Delta x},\dfrac{l}{N'\Delta y}\right)$ of the APSD of the surface under study. The Hann weighting function (16) was used

$$w(x_{m'},y_{n'})=\cos^2\left(\pi\frac{m'-M'/2}{M'}\right)\cos^2\left(\pi\frac{n'-N'/2}{N'}\right) \tag{16}$$

for each sub-domain to suppress the leakage of its spectrum. The minimum sampling interval of the surfaces measured by the optical profilometer MicroProf FRT is $\Delta x = \Delta y = 2$ μm. Hence, it is not possible to distinguish the surface details corresponding to the spatial frequencies $f_x \ge 1/2M'$ (1/μm), $f_y \ge 1/2N'$ (1/μm). So, the upper frequency limit of surface topography measurements is $1{,}7\times10^{-3}$ (1/m) for

both frequencies $f_x$, $f_y$. These limitations should be considered when the results are interpreted.

### 5.1
### Influence of water pressure variation

First the results for two selected values of the water pressure (for the constant values $m_a$ = 500 g/min, $v$ = 70 mm/min) are compared (see Fig. 5 - Fig. 12). A half-width of the main peak of the normalized RPSD within the individual surface zones is studied to find a quantitative parameter characterizing the variations in the APSD of the surface under study. Values found are presented in Tab. 2. It is obvious from Tab. 2 that the half-width of the normalized RPSD peak does not significantly change with the water pressure variations within the smooth zone. The half-width of the normalized RPSD peak is wider for higher water pressures. Another way to characterize the variations in APSD of the studied surface can be the AnPSD utilization. The angular coordinate $\theta$ of a maximum of the normalized AnPSD is monitored within the individual surface zones. Values found are presented in Tab. 3. It should be noted that the maxima of the normalized AnPSD are relatively flat, i.e. the significant fluctuations in their values can be observed.

**Table 2** Half-width of the normalized RPSD peak (influence of water pressure variation)

| Zones | Smooth | | Rough | |
|---|---|---|---|---|
| Water pressure, MPa | 200 | 350 | 200 | 350 |
| Half-width of the peak, 1/m | 289,4 | 287,5 | 437,3 | 535,6 |
| Relative difference, % | 0,0 | | 20,2 | |

**Table 3** Angular coordinate $\theta$ of the normalized AnPSD maximum (influence of water pressure variation)

| Zones | Smooth | | Rough | |
|---|---|---|---|---|
| Water pressure, MPa | 200 | 350 | 200 | 350 |
| Coordinate $\theta$ of the maximum, ° | 48,0 | 48,0 | 19,2 | 6,6 |
| Relative difference, % | 0,0 | | 97,7 | |

It can be seen from Tab. 3 that no changes of the angular coordinate $\theta$ of the normalized AnPSD maximum occur with the water pressure change within the smooth zone. However the displacement of the maximum angular coordinate of normalized AnPSD is significant in the case of the rough zone. It can be seen from values of $\theta$ in Tab. 3 that the curvature of waterjet surface striation within the rough zone is higher for the lower water pressure.

### 5.2
### Influence of abrasive mass flow rate

Now the results for two selected values of the abrasive flow rate (for constant values $p$ = 200 MPa, $v$ = 70 mm/min) will be compared. For further explanation the presentation of digital maps of the studied surfaces and images of their APSD, normalized RPSD and normalized AnPSD will be omitted. The half-width of the normalized RPSD peaks and the angular coordinate $\theta$ of the normalized AnPSD maxima of surfaces under study will be determined likewise in the case of the water pressure variation. It can be seen from Tab. 4 that the half-width of the normalized RPSD peak does not change significantly with the variation of the abrasive flow rate within the smooth and rough zone.

Tab. 5 shows that the angular coordinate $\theta$ of the normalized AnPSD maximum is the same for both values of the abrasive flow rate being studied within the smooth zone.

**Table 4** Half-width of the normalized RPSD peak (influence of abrasive flow rate variation)

| Zones | Smooth | | Rough | |
|---|---|---|---|---|
| Abrasive flow rate, g/min | 300 | 500 | 300 | 500 |
| Half-width of the peak, 1/m | 293,4 | 289,4 | 440,4 | 437,3 |
| Relative difference, % | 1,4 | | 0,7 | |

**Table 5** Angular coordinate $\theta$ of the normalized AnPSD maximum (influence of abrasive flow rate variation)

| Zones | Smooth | | Rough | |
|---|---|---|---|---|
| $m_a$ /g/min | 300 | 500 | 300 | 500 |
| Coordinate $\theta$ of the maximum, ° | 48,0 | 48,0 | 25,2 | 19,2 |
| Relative difference, % | 0,0 | | 27,0 | |

It is observed within the rough zone that the coordinate $\theta$ of the normalized AnPSD maximum is lower for the higher abrasive flow rate. It means that the curvature of the surface striation is higher within the rough zone at the lower abrasive flow rate.

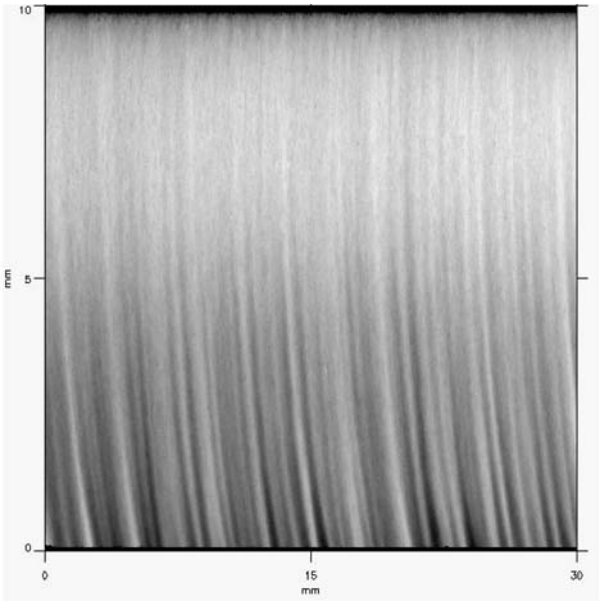


**Figure 5** Digital map of the surface for the water pressure of 200 MPa (measured by MicroProf FRT)

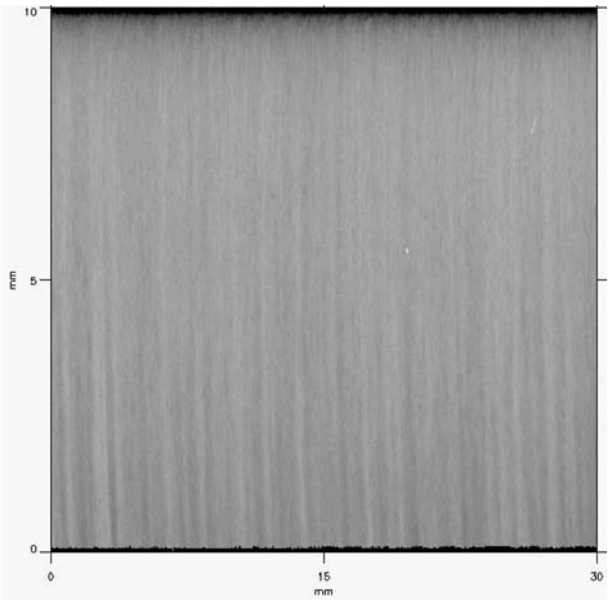


**Figure 6** Digital map of the surface for the water pressure of 350 MPa (measured by MicroProf FRT)

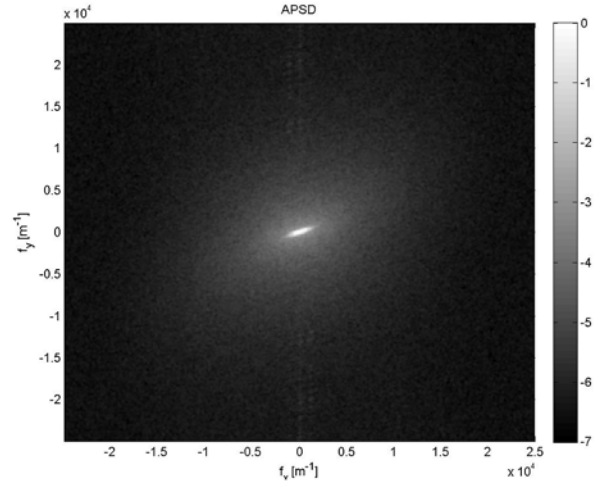


**Figure 7** Normalized areal power spectral density of the surface obtained from Fig. 5 (water pressure 200 MPa) – semilogarithm scale

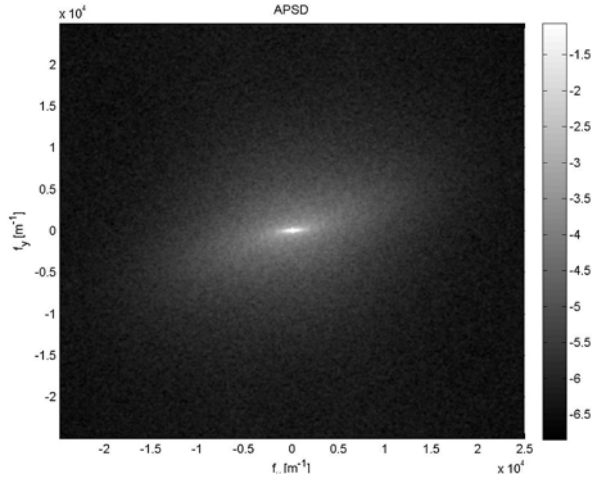


**Figure 8** Normalized areal power spectral density of the surface obtained from Fig. 6 (water pressure 350 MPa) - semilogarithm scale

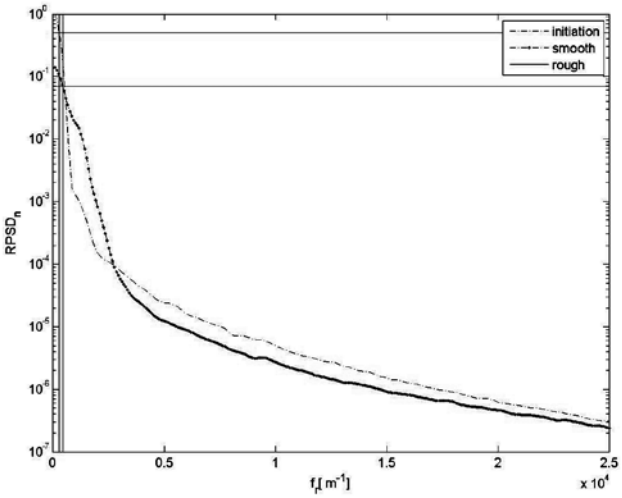


**Figure 9** Normalized radial power spectral density of the surface obtained from Fig. 5 (water pressure 200 MPa) – semilogarithm scale

## 5.3
## Influence of abrasive mass flow rate

Here the results for two selected values of the AWJ traverse speed (for constant values $p$ = 200 MPa, $m_a$ = 500 g/min) will be compared. The values of the half-width of the normalized RPSD peak are almost the same within the smooth zone in this case (Tab. 6). The significant difference

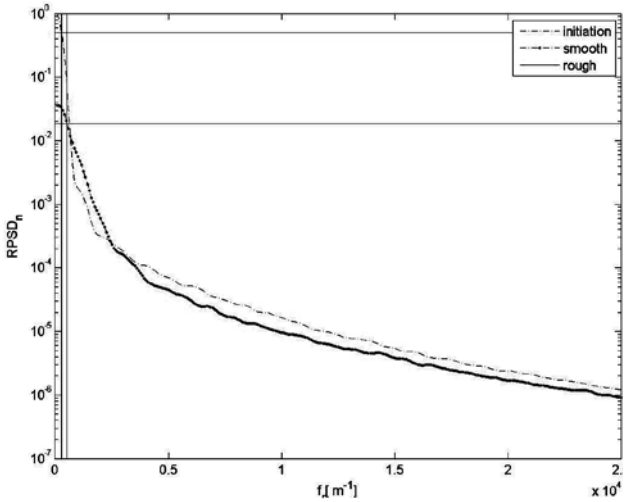


**Figure 10** Normalized radial power spectral density of the surface obtained from Fig. 6 (water pressure 350 MPa) – semilogarithm scale

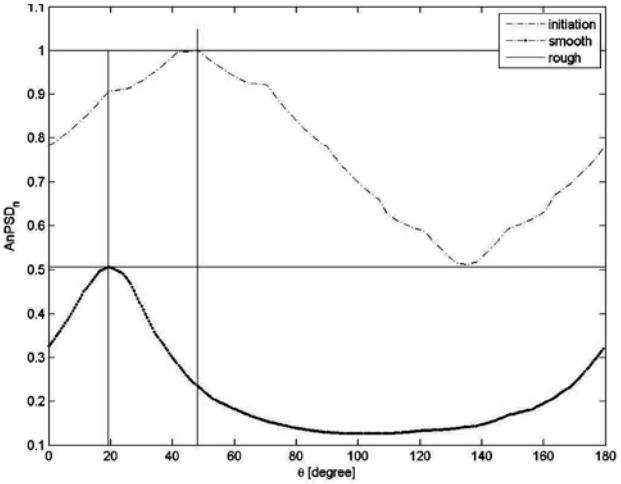


**Figure 11** Normalized angular power spectral density of the surface from Fig. 5 – semilogarithm scale

between the half-width of the peak occurs within the rough zone case. The half-width of the normalized RPSD peak is wider at the lower traverse speed of the cutting head.

**Table 6** Half-width of the normalized RPSD peak (influence of the AWJ head velocity)

| Zones | Smooth | | Rough | |
|---|---|---|---|---|
| $v$ /mm/min | 70 | 120 | 70 | 120 |
| Half-width of the peak, 1/m | 287,5 | 289,2 | 535,6 | 324,9 |
| Relative difference, % | 0,6 | | 49,0 | |

As evidenced by Tab. 7, the angular position of the normalized AnPSD maximum is the same for both values of the traverse speed selected within the smooth zone. Within the rough zone the coordinate $\theta$ of the normalized AnPSD maximum is higher when the higher AWJ head velocity is utilized. It means that the curvature of the surface striation within the rough zone is greater at the higher traverse speed of the cutting head.

**Table 7** Angular coordinate θ of the normalized AnPSD maximum (influence of the AWJ head velocity)

| Zones | Smooth | | Rough | |
|---|---|---|---|---|
| $v$ /mm/min | 70 | 120 | 70 | 120 |
| Coordinate $\theta$ of the maximum, ° | 48,0 | 48,3 | 6,6 | 11,4 |
| Relative difference, % | 0,6 | | 53,3 | |

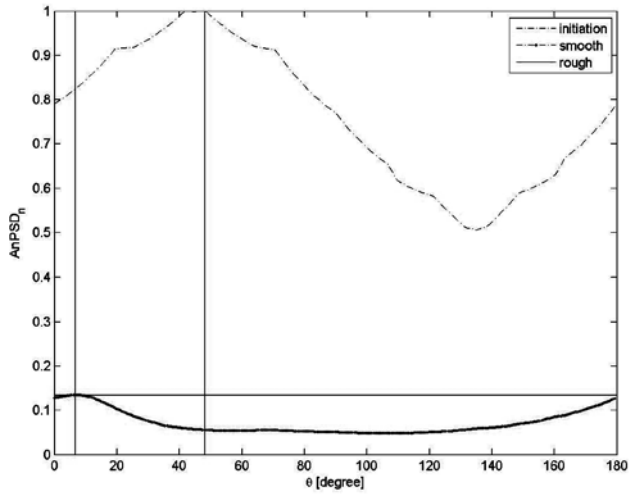


**Figure 12** Normalized angular power spectral density of the surface from Fig. 6 – semilogarithm scale

## 6 Conclusions

This paper presents the results of applying the areal spectral analysis to selected surfaces generated by AWJ cutting and measured by means of the optical profilometer MicroProf FRT. The main notions concerning the areal spectral analysis are introduced. It is followed by the discussion of the measurement procedure limitations, and the unavoidable distortions in numerical results are pointed out. The RPSD and AnPSD are used for the quantitative evaluation of the surface topography. These two quantities were derived from the ASPD being estimated by the periodogram method in combination with the Welch´s method. The changes within the RPSD and/or AnPSD are quantitatively characterized by means of the half-width of the normalized RPSD peak and/or the angular coordinate of the maximum of the normalized AnPSD. The conclusions following from the comparison of the results obtained for the selected values of technological parameters (pressure of water at the input of the AWJ head, abrasive flow rate, and traverse speed of the AWJ cutting head) of the aforementioned surfaces can be summarized as follows (see Tabs 2-7). There are no significant changes observed in the half-width of the normalized RPSD peak or the angular coordinate of the maximum of the normalized AnPSD within the smooth zone of the surfaces under study within all the values of the technological parameters being monitored. The significant changes in the mentioned parameters were observed within the rough zone of the surfaces being studied:

- The half-width of the normalized RPSD peak increases with the increase of the water pressure at the input of the AWJ cutting head. It means that the spectral power of the surface extends to higher spatial frequencies (higher spatial frequencies become more significant).
- The half-width of the normalized RPSD peak does not change with the change of the abrasive flow rate. The spectral power distribution of the surface is not affected by possible variations in the abrasive flow rate.
- The half-width of the normalized RPSD peak decreases with the increase of the traverse speed of the cutting head. The spectral power density of the surface moves to the lower spatial frequencies (lower spatial frequencies become more significant).
- The angular coordinate of the maximum of the normalized AnPSD decreases very significantly with the increase of the water pressure at the input of the AWJ cutting head. Greater curvature of the surface striation within the rough zone is obtained by using lower water pressure. This result indicates that the higher the water pressure, the more easily the water jet cuts the samples. This conclusion must be proved by a more detailed research with an even higher number of samples.
- The angular coordinate of the maximum of the normalized AnPSD significantly decreases with the increase of the abrasive flow rate. Alike in the previous case the curvature of the surface striation within the rough zone is greater by using the lower abrasive flow rate. It could be interpreted in the way that the water jet loses its kinetic energy markedly within the upper part of the cutting wall at the higher traverse speed of the cutting head.
- The angular coordinate of the maximum of the normalized AnPSD significantly increases with the increase of the traverse speed of the AWJ cutting head (the curvature of the surface striation within the rough zone is greater at the higher traverse speed of the cutting head). It means that the water jet loses its kinetic energy markedly within the upper part of the cutting wall at the higher traverse speed of the cutting head.

It is possible to conclude that the spectral analysis of surfaces generated by AWJ can provide the results useful for the surface topography characterization. The main advantage of this technique with respect to topography parameters usually utilized in that case consists in a different view of the surface topography characterization. Particularly it allows quantitative evaluating directions of surface irregularities orientation within individual zones of the surfaces.

### Acknowledgements

This work was supported by the Grant Agency of the Czech Republic under contract No. 101/09/0650 and by the Ministry of Education, Youth and Sports of the Czech Republic under contracts MSM 0021630518, MSM6198910016, projects BD13101017, RMTVC No. CZ.1.05/2.1.00/01.0040 and the IT4Innovations Centre of Excellence project, reg. no. CZ.1.05/1.1.00/02.0070.

## 7 References

[1] Valíček, J.; Hloch, S.; Kozak, D. Surface geometric parameters proposal for the advanced control of abrasive waterjet technology. // The International Journal of Advanced Manufacturing Technology. 41, 3-4(2009), pp. 323-328.

[2] Valíček, J.; Hloch, S. Optical measurement of surface and topographical parameters investigation created by abrasive waterjet. International Journal of Surface Science and Engineering. 3, 4(2009), pp. 360-373. DOI: 10.1504/IJSURFSE.2009.02[421.

[3] Valíček, J. et al. An investigation of surfaces generated by abrasive waterjets using optical detection. // Strojniski vestnik-Journal of mechanical engineering. 53, (2007), pp. 224-232.

[4] Hloch, S., Valíček, J. Prediction of distribution relationship of titanium surface topography created by abrasive waterjet. // International Journal of Surface Science and Engineering. 5,

2/3(2011), pp. 152-168.
DOI. 10.1504/IJSURFSE.2011.041399
[5] Hloch, S.; Valíček, J. Topographical anomaly on surfaces created by abrasive waterjet. // The International Journal of Advanced Manufacturing Technology.
DOI: 10.1007/s00170-011-3511-3
[6] Hashish, M. A. Model study of metal cutting with abrasive water jet. // ASME J Engng Mat and Techn, 106, (1984), pp. 88–100.
[7] Arola, D.; Ramulu, M. Material removal in abrasive waterjet machining of metals surface integrity and texture. // Wear, 210, 1/2(1997), pp. 50–58
[8] Thomas, D. J. Characteristics of abrasive waterjet cut-edges and the affect on formability and fatigue performance of high strength steels. // Journal of Manufacturing Processes, 11, (2009), pp. 97-105. ISSN 0268-3768.
[9] Kong, M. C., et al. Aspects of material removal mechanism in plain waterjet milling on gamma titanium aluminide. // Journal of Materials Processing Technology, 210, (2010), pp. 573-584. ISSN 0924-0136.
[10] Ma, C.; Deam, R. T. A correlation for predicting the kerf profile from abrasive water jet cutting. // Experimental Thermal and Fluid Science, 30, (2006),p p. 337-343.
[11] Brigham, E. O. The Fast Fourier Transform and its application, Prentice-Hall, Upper Saddle River, 1988.
[12] Bracewell, R.N. The Fourier Transform and its Applications, 3rd ed., McGraw-Hill Companies, Boston, 2000.
[13] Mainsah, E.; Greenwood, J. A.; Chetwynd, D. G. Metrology and Properties of Engineering Surfaces, Kluwert Academic Publishers, Dordrecht, 2001.

**Authors' addresses**

***Kateřina Brillová***
*I*nstitute of Physical Engineering
Brno University of Technology
Technická 2896/2
616 69 Brno
Czech Republic

***Miloslav Ohlídal***
Institute of Physical Engineering
Brno University of Technology
Technická 2896/2
616 69 Brno
Czech Republic

***Jan Valíček***
Institute of Physics, Faculty of Mining and Geology
RMTVC, Faculty of Metallurgy and Materials Engineering,
VŠB - Technical University of Ostrava
17 Listopadu
708 33 Ostrava – Poruba
Czech Republic
jan.valicek@vsb.cz

***Dražan Kozak***
Mechanical Engineering Faculty in Slavonski Brod
J. J. Strossmayer University of Osijek
Trg Ivane Brlić Mažuranić 2
HR – 35000 Slavonski Brod
Croatia

***Sergej Hloch***
Faculty of Manufacturing Technologies of Technical University of Košice with a seat in Prešov
Bayerova 1
080 01 Prešov
Slovak Republic

***Michal Zeleňák***
Institute of Physics
Faculty of Mining and Geology
VŠB - Technical University of Ostrava
17 Listopadu
708 33 Ostrava – Poruba
Czech Republic

***Marta Harničárová***
Nanotechnology Centre
VŠB -Technical University of Ostrava
17 Listopadu
708 33 Ostrava – Poruba
Czech Republic

***Petr Hlaváček***
Institute of Physics
Faculty of Mining and Geology
VŠB - Technical University of Ostrava
17 Listopadu
708 33 Ostrava – Poruba
Czech Republic